The evolution of perturbations

Milestone III, AST5220
Spring 2020

Jowita Borowska

Code available at: https://github.com/jowborowska/AST5220

1 Introduction

The two former project milestones focused on determining the background cosmology of the Universe. Now, we will consider "the anisotropies in the cosmic distribution of photons and inhomogenities in the matter" (Dodelson, 2003). We will follow the behaviour of perturbations to the metric (Ψ, Φ), density (δ_b, δ_{cdm}) and velocity (v_b, v_{cdm}) of baryons and dark matter, as well as perturbations to the photons, expanded in multipoles (Θ_ℓ). The evolution of these perturbations is governed by the Boltzmann equations for the components of interest (baryonic matter, cold dark matter and photons), in addition to the Einstein equations for the gravitational potentials. A more thorough description of all the quantities and equations of inerest will be presented in the Methods section, together with the details of numerical implementation. Therafter, we will show and discuss results produced by the programs (Results section).

2 Methods

2.1 Quantities of interest

Throughout the project, we will be using logarithm of the scale factor, $x = \ln(a)$, as the time variable. As we consider the inhomogeneous Universe, all the quantities of interest depend not only on time, but also on the position in space. We will be working in Fourier space, using the wavevector, $\vec{k}$ - Fourier transformed variable of the position. Moreover, the evolution of a mode associated with a given wavevector depends only on its magnitude, $k = |\vec{k}|$. We have then a set of quantities of interest: $\Psi(x,k)$, $\Phi(x,k)$, $\delta_{cdm}(x,k)$, $\delta_b(x,k)$, $v_{cdm}(x,k)$, $v_b(x,k)$ and $\Theta_\ell(x,k)$, that we want to compute from the early times (with corresponding scale factor $a_{min}(t) = 10^{-7} \Rightarrow x_{min} = \ln(10^{-7})$) until today ($a(t_0) = a_0 = 1 \Rightarrow x_0 = 0$) for six different k-values, chosen to be 0.0005/Mpc, 0.001/Mpc, 0.005/Mpc, 0.01/Mpc, 0.1/Mpc and 0.15/Mpc. Definitions of all the quantities, following Dodelson (2003) and Callin (2006), can be found below.

Perturbations to the metric - Ψ, Φ

The smooth, expanding, flat universe can be described by the Friedmann-Robertson-Walker (FRW) metric,

$$g_{\mu\nu} = \begin{pmatrix} -1 & 0 & 0 & 0 \\ 0 & a^2 & 0 & 0 \\ 0 & 0 & a^2 & 0 \\ 0 & 0 & 0 & a^2 \end{pmatrix}, \tag{1}$$

where $a = a(t)$ is the scale factor, that depends only on time. Using Newtonian gauge, we can introduce perturbations to the metric, so that it takes a more complicated form,

$$g_{\mu\nu} = \begin{pmatrix} -(1+2\Psi) & 0 & 0 & 0 \\ 0 & a^2(1+2\Phi) & 0 & 0 \\ 0 & 0 & a^2(1+2\Phi) & 0 \\ 0 & 0 & 0 & a^2(1+2\Phi) \end{pmatrix}, \tag{2}$$

where the functions $\Psi = \Psi(\vec{x}, t)$ and $\Phi = \Phi(\vec{x}, t)$ depend both on space and time. Φ is the perturbation to the spatial curvature and Ψ corresponds to the Newtonian potential.

Nonrelativistic matter - δ_{cdm}, δ_b, v_{cdm}, v_b

Both cold dark matter and baryons are not uniformly distributed in the Universe. The spatial differences in density of these components are characterized by fractional overdensities,

$$\delta(\vec{x}, t) = \frac{\rho(\vec{x}, t) - \overline{\rho}(t)}{\overline{\rho}(t)}, \tag{3}$$

where $\rho(\vec{x}, t)$ is the density at a given position $\vec{x}$ and time t, whereas $\overline{\rho}(t)$ is the average density at that time. We have then $\delta_{cdm}(\vec{x}, t)$ and $\delta_b(\vec{x}, t)$, consecutively for cold dark matter (CDM) and baryonic matter. There are also velocities associated with both dark matter, $\vec{v}_{cdm}(\vec{x}, t)$, and baryons, $\vec{v}_b(\vec{x}, t)$. The only relevant components of the Fourier transformed velocities are the ones parallel to the wavevector (so that we will be working with scalar velocities).

Photons - Θ_ℓ

Perturbations to the photons are associated with the relative variation of the photon temperature, $\delta T/T$ (additional polarization effects will not be included in this project). We have a monopole perturbation, being equivalent of the "energy overdensity", $\delta_\gamma = 4\Theta_0$, and a dipole, equivalent of the velocity of the fluid due to the Doppler effect, $v_\gamma = -3\Theta_1$. However, since photons are relativistic, they have also higher multipole moments, so that we need more quantities to characterize their distribution. In addition to position, $\vec{x}$, and time, t, the photon distribution depends also on the momentum of the photon, $\vec{p}$ (in particular, its direction of propagation). Photon perturbations can then be described either by the variable $\Theta(k, \mu, t)$ - Fourier transform of $\delta T/T$, where $\mu = \frac{\vec{k}\cdot\vec{p}}{kp}$, or a set of multipole moments of the temperature field, $\Theta_\ell(k, t)$. The l-th moment is defined as

$$\Theta_\ell(k, t) = \frac{i^l}{2} \int_{-1}^{1} \mathcal{P}_l(\mu)\Theta(\mu)d\mu, \tag{4}$$

where $\mathcal{P}_\ell(\mu)$ are the Legendre polynomials of order ℓ, so that the higher moments correspond to the smaller scale structure of the temperature field. The previously mentioned monopole is the zeroth moment, and dipole - the first moment.

2.2 Equations governing the evolution of perturbations

We will follow Callin (2006) and Winther (2020) in order to present the entire set of coupled equations governing the evolution of the quantities described in the previous subsection. We include Boltzmann equations for photons, CDM and baryons, as well as the ones for both gravitational potentials, given by the Einstein equation. Here, we will use some of the precomputed quantities that were thoroughly described in the previous milestones (like Hubble parameter or optical depth and its derivatives).

Since the system of equations is numerically unstable at early times due to the tight coupling between photons and baryons, we must apply some approximations and consider two regimes. At the beginning, the optical depth is very large, so that the electrons observe only the temperature fluctuations in their close vicinity, i.e. only very smooth fluctuations (system is in thermodynamic equilibrium and all gradients are washed out). Therefore, the monopole, Θ_0, and the dipole, Θ_1, are the only relevant multipole moments of the temperature field in the tight coupling regime. As the Universe expands, the fluid becomes thinner and the optical depth decreases - electrons are able to see "further away". They become more sensitive to the higher order multipoles, so that after the tight coupling regime ends we will keep track of Θ_0, Θ_1, ..., $\Theta_{\ell_{max}}$, with a cutoff at $\ell_{max} = 7$.

We stay in the tight coupling regime as long as $|\tau'| > 10 \cdot \min(1, \frac{ck}{\mathcal{H}})$ and switch to the full system of equations no later than at the start of recombination ($z = 1700 \Rightarrow x \approx -7.44$).

Initial conditions

At the beginning of the integration (in the tight coupling regime), we have

$$\Psi = -\frac{2}{3} \tag{5}$$

$$\Phi = -\Psi \tag{6}$$

$$\delta_{cdm} = \delta_b = -\frac{3}{2}\Psi \tag{7}$$

$$v_{cdm} = v_b = -\frac{ck}{2\mathcal{H}}\Psi \tag{8}$$

$$\Theta_0 = -\frac{1}{2}\Psi \tag{9}$$

$$\Theta_1 = +\frac{ck}{6\mathcal{H}}\Psi. \tag{10}$$

After switching to the full system, we use the last results of the quantities computed in the tight coupling regime as the new initial values. For the multipoles that were not included in the tight coupling regime, we use

$$\Theta_2 = -\frac{20ck}{45\mathcal{H}\tau'}\Theta_1 \tag{11}$$

$$\Theta_\ell = -\frac{\ell}{2\ell+1}\frac{ck}{\mathcal{H}\tau'}\Theta_{\ell-1} \qquad 2 < \ell \leq 7. \tag{12}$$

Equations of interest

$$\Psi = -\Phi - \frac{12H_0^2\Omega_{r,0}\Theta_2}{c^2k^2a^2} \tag{13}$$

$$\Phi' = \Psi - \frac{c^2k^2}{3\mathcal{H}^2}\Phi + \frac{H_0^2}{2\mathcal{H}^2}\left[\Omega_{cdm,0}a^{-1}\delta_{cdm} + \Omega_{b,0}a^{-1}\delta_b + 4\Omega_{r,0}a^{-2}\Theta_0\right] \tag{14}$$

$$\delta'_{\rm CDM} = \frac{ck}{\mathcal{H}}v_{\rm CDM} - 3\Phi' \tag{15}$$

$$\delta'_b = \frac{ck}{\mathcal{H}}v_b - 3\Phi' \tag{16}$$

$$v'_{\rm CDM} = -v_{\rm CDM} - \frac{ck}{\mathcal{H}}\Psi \tag{17}$$

$$R = \frac{4\Omega_{r,0}}{3\Omega_{b,0}a} \tag{18}$$

$$q = \frac{-[(1-R)\tau' + (1+R)\tau''](3\Theta_1 + v_b) - \frac{ck}{\mathcal{H}}\Psi + (1-\frac{\mathcal{H}'}{\mathcal{H}})\frac{ck}{\mathcal{H}}(-\Theta_0 + 2\Theta_2) - \frac{ck}{\mathcal{H}}\Theta'_0}{(1+R)\tau' + \frac{\mathcal{H}'}{\mathcal{H}} - 1} \tag{19}$$

$$v'_b = \begin{cases} \frac{1}{1+R}\left[-v_b - \frac{ck}{\mathcal{H}}\Psi + R(q + \frac{ck}{\mathcal{H}}(-\Theta_0 + 2\Theta_2) - \frac{ck}{\mathcal{H}}\Psi)\right] & \text{(in the tight coupling regime)} \\ -v_b - \frac{ck}{\mathcal{H}}\Psi + \tau' R(3\Theta_1 + v_b) & \text{(in the second regime)} \end{cases} \tag{20}$$

$$\Theta'_0 = -\frac{ck}{\mathcal{H}}\Theta_1 - \Phi', \tag{21}$$

$$\Theta'_1 = \begin{cases} \frac{1}{3}(q - v'_b) & \text{(in the tight coupling regime)} \\ \frac{ck}{3\mathcal{H}}\Theta_0 - \frac{2ck}{3\mathcal{H}}\Theta_2 + \frac{ck}{3\mathcal{H}}\Psi + \tau'\left[\Theta_1 + \frac{1}{3}v_b\right] & \text{(in the second regime)} \end{cases} \tag{22}$$

$$\tag{23}$$

The higher multipoles are expressed directly in terms of the lower ones in the tight coupling regime,

$$\Theta_2 = -\frac{20ck}{45\mathcal{H}\tau'}\Theta_1 \tag{24}$$

$$\Theta_\ell = -\frac{\ell}{2\ell+1}\frac{ck}{\mathcal{H}\tau'}\Theta_{\ell-1}, \qquad 2 < \ell \leq 7 \tag{25}$$

whereas after the end of tight coupling we use,

$$\Theta'_\ell = \frac{\ell ck}{(2\ell+1)\mathcal{H}}\Theta_{\ell-1} - \frac{(\ell+1)ck}{(2\ell+1)\mathcal{H}}\Theta_{\ell+1} + \tau'\left[\Theta_\ell - \frac{1}{10}\Theta_2\delta_{\ell,2}\right], \qquad 2 \leq \ell < 7 \tag{26}$$

$$\Theta'_\ell = \frac{ck}{\mathcal{H}}\Theta_{\ell-1} - c\frac{\ell+1}{\mathcal{H}\eta(x)}\Theta_\ell + \tau'\Theta_\ell, \qquad \ell = 7. \tag{27}$$

$$\tag{28}$$

2.3 Source function

Instead of performing the multipole expansion of the photon perturbation variable first and then integrating the hierarchies of equations, we can start by integrating the equation for $\dot{\Theta}$ and subsequently expand the result in multipoles (Callin, 2006). This technique is called the line-of-sight integration. With x as the time variable, we get

$$\Theta_\ell(k, x=0) = \int_{-\infty}^{0} \tilde{S}(k,x) j_\ell[k(\eta_0 - \eta(x))] dx, \tag{29}$$

where j_ℓ-s are the spherical Bessel functions and $\tilde{S}(k,x)$ is the source function, defined as

$$\tilde{S}(k,x) = \tilde{g}\left[\Theta_0 + \Psi + \frac{1}{4}\Theta_2\right] + e^{-\tau}\left[\Psi' - \Phi'\right] - \frac{1}{ck}\frac{d}{dx}(\mathcal{H}\tilde{g}v_b) + \frac{3}{4c^2k^2}\frac{d}{dx}\left[\mathcal{H}\frac{d}{dx}(\mathcal{H}\tilde{g}\Theta_2)\right]. \tag{30}$$

The last term in the expression above can be written as

$$\frac{d}{dx}\left[\mathcal{H}\frac{d}{dx}(\mathcal{H}\tilde{g}\Theta_2)\right] = \frac{d(\mathcal{H}\mathcal{H}')}{dx}\tilde{g}\Theta_2 + 3\mathcal{H}\mathcal{H}'(\tilde{g}'\Theta_2 + \tilde{g}\Theta_2') + \mathcal{H}^2(\tilde{g}''\Theta_2 + 2\tilde{g}'\Theta_2' + \tilde{g}\Theta_2''). \tag{31}$$

2.4 Numerical implementation

The third project milestone is based on modifying the Perturbations class in the corresponding files from the given set of C++ templates. To create the class object, we have to provide it with the objects of BackgroundCosmology and RecombinationHistory classes, in order to fetch the quantities computed in the previous milestones, that occur in our equations to solve.

The class Perturbations has several functions. The main part of the program is contained within the function integrate_perturbations(). Here, we set up an array of 100 logarithmically spaced k-values from $k_{min} = 0.00005$/Mpc to $k_{max} = 0.3$/Mpc and a grid of 1000 equally spaced x-values in range $x \in [\ln(10^{-7}), 0]$, as well as arrays for storing $100 \cdot 1000$ values of all the quantities of interest that will be computed. We solve the entire set of equations for all the combinations of x and k (using an outer for loop through all k-values), to finally spline the results. The quantities of interest at a given time are stored as a vector on the form $\vec{y}(x,k) = (\delta_{cdm}, \delta_b, v_{cdm}, v_b, \Phi, \Theta_0, \Theta_1, \Theta_2, ..., \Theta_7)$, so it is important to keep track of the indices corresponding to a given quantity. As described in the section 2.2, we consider two regimes - for each we set up a separate ordinary differential equation solver. We have then two functions for implementing the initial conditions (set_ic() and set_ic_after_tight_coupling()), as well as two functions for creating the right hand side of the system of ordinary differential equations to solve (rhs_tight_coupling_ode() and rhs_full_ode()). In order to determine the time of switching from the tight coupling approximation to the full system, we implement the 3-part condition inside the get_tight_coupling_time() function. After gathering the results from both solvers, we can combine the two regimes and fill part of the initially created arrays of the quantities $\delta_{cdm}, \delta_b, v_{cdm}, v_b, \Phi, \Theta_0, \Theta_1, \Theta_2, ..., \Theta_7$, corresponding to a given wavenumber. Then, we repeat the process for all the 100 k-values to complete the arrays. Thereafter, we can compute the dynamical variable, Ψ, for all k and x combinations and fill the corresponding array entirely. Finally, we create the 2D splines of all the quantities through the resulting data points.

After integrating the perturbations, we can compute the source function (Eq. 30) with use of compute_source_functions() method. We have also series of "get" functions, used to return all the quantities of interest (employing splines). Function info() prints out the information about the model and function output() writes the data to a file for a given k-value, specified in the Main.cpp file. Running the whole script takes over 18 seconds, with the majority of time spent on the integration part of the program (17 s).

The generated text files with data corresponding to given wavenumbers are thereafter read by a program written in Python (milestone3.py), also used to create all the plots included in

this report. Codes to the programs (Perturbations.h, Perturbations.cpp, milestone3.py) are available in the following github repository: https://github.com/jowborowska/AST5220

3 Results

We have generated six datasets with different wavenumbers - two corresponding to the large scales ($k = 0.0005$/Mpc and $k = 0.001$/Mpc), two for the intermediate scales ($k = 0.005$/Mpc and $k = 0.01$/Mpc) and two for the small scales ($k = 0.1$/Mpc and $k = 0.15$/Mpc).

Figure 1. shows the behaviour of gravitational potentials, Φ and Ψ - perturbations to the metric. We can clearly see that their magnitude is similar, so that the sum, $\Phi + \Psi$, is very small (close to zero) at all times. In the beginning, all the modes are outside the horizon and the potential, Φ, is constant. From the plots we can conclude that for the smaller scale modes horizon crossing happens earlier, i.e. the mode associated with $k = 0.15$/Mpc enters the horizon much earlier than the one associated with $k = 0.01$/Mpc (intermediate scale) or $k = 0.001$/Mpc (large scale). As computed in the first project milestone, the matter-radiation equality occurs around $x \approx -8.5$. The smallest scale modes enter the horizon well before that. Therafter, at later times, all the modes evolve similarly again.

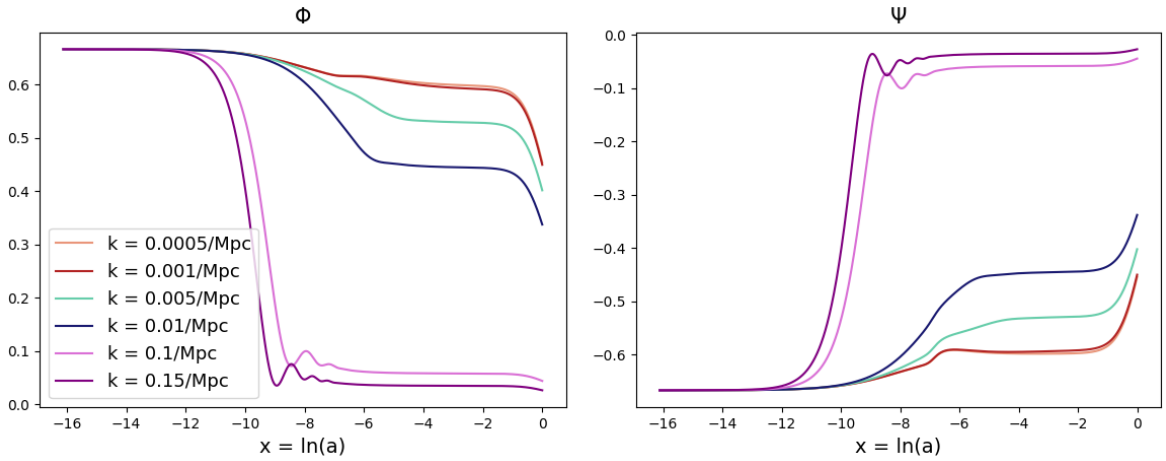

Figure 1: Perturbations to the metric plotted as a function of logarithm of the scale factor, x, for six different values of the wavenumber, k.

The evolution of fractional matter overdensities is shown on Figure 2. We will first look at the left panel, corresponding to the cold dark matter. As before, all the modes have the same, constant value at the beginning. Then, the amplitude increases as the modes enter horizon at different times. At late times (when all the modes are inside the horizon), the density perturbation grows proportional to the scale factor. For the small scale modes, that enter the horizon before the matter-radiation equality ($k = 0.15$/Mpc and $k = 0.1$/Mpc), the growth of overdensity is slower between horizon entry and matter-radiation equality than in the matter-dominated era. This is called the Meszaros effect. The earlier the horizon entry, the more suppression a given mode undergoes. The evolution of density perturbation to the baryonic matter (Figure 2, right panel) looks quite similar for the modes associated with intermediate and large scales. However, we can clearly see some oscillations in the baryonic fluid for the modes with higher wavenumbers in approximately the same time period as the

suppressed growth of δ_{cdm} takes place. At early times, when the photons are tightly coupled to the baryons, "the pressure of photons supports oscillations on small scales". In that time the CDM overdensity grows, so that after decoupling we have $\delta_{cdm} > \delta_b$. Therafter, the baryons fall into the potential wells sourced by the dark matter, so that $\delta_b \to \delta_c$ (Baumann).

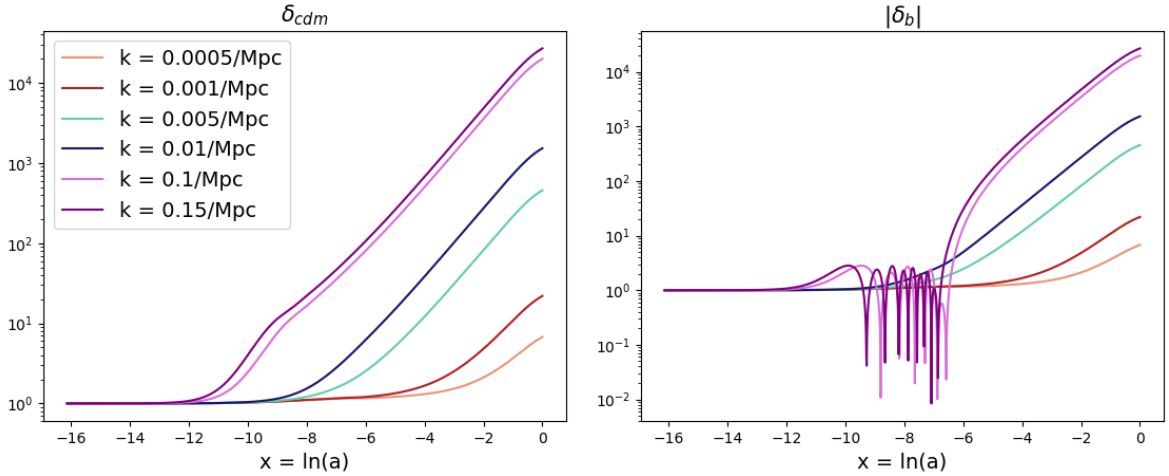

Figure 2: The density perturbation of cold dark matter (left panel) and baryons (right panel) plotted as a function of logarithm of the scale factor, x, for six different values of the wavenumber, k. Logarithmic y-axis has been used.

Figure 3 shows the velocity components parallel to the wavevectors for the cold dark matter (left panel) and baryons (right panel). The evolution, that we can observe, is somewhat similar to the one displayed by the density perturbations. The small scale modes are associated with higher velocity values, but the curves seem to converge at later times.

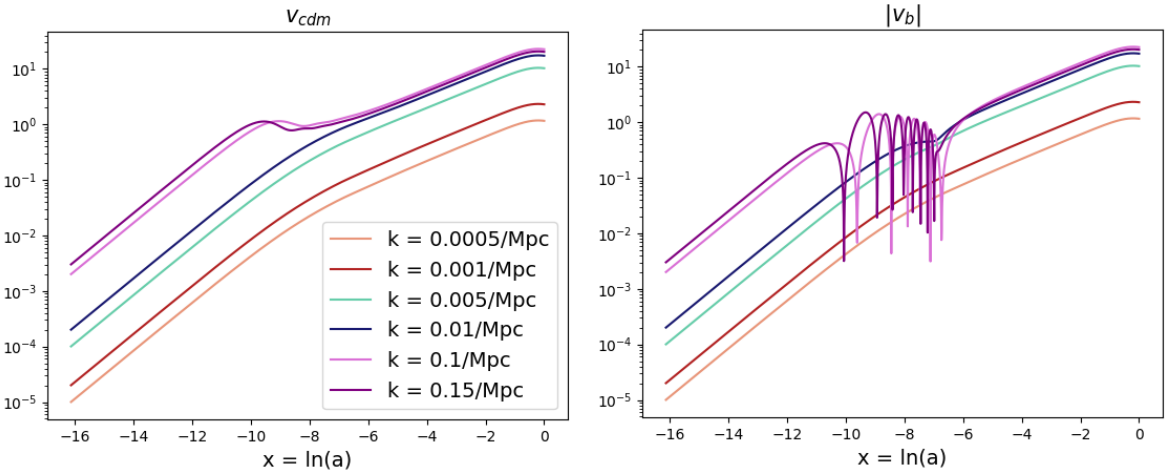

Figure 3: The velocity of cold dark matter (left panel) and baryons (right panel) plotted as a function of logarithm of the scale factor, x, for six different values of the wavenumber, k. Logarithmic y-axis has been used.

Figures 4 and 5 show the evolution of perturbation to the radiation. Here, we can clearly see that the large scale modes are not very much affected, intermediate scales undergo a few oscillations and the multipoles associated with the small scales start to oscillate early, with damping at later times. We can observe that for the smallest scales, the damping begins earlier - prior to decoupling (diffusion damping). The acoustic oscillations that we can observe give rise to the peaks in the spectrum of CMB anisotropies (Baumann).

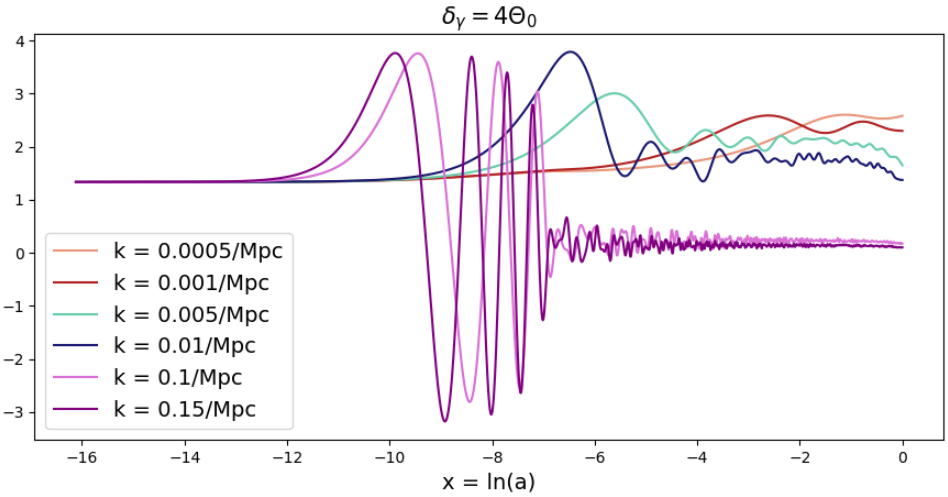

Figure 4: Perturbation to the photons - energy density, being 4 times the zeroth multipole moment of the temperature field (monopole), $\delta_\gamma = 4\Theta_0$, plotted as a function of logarithm of the scale factor, x, for six different values of the wavenumber, k.

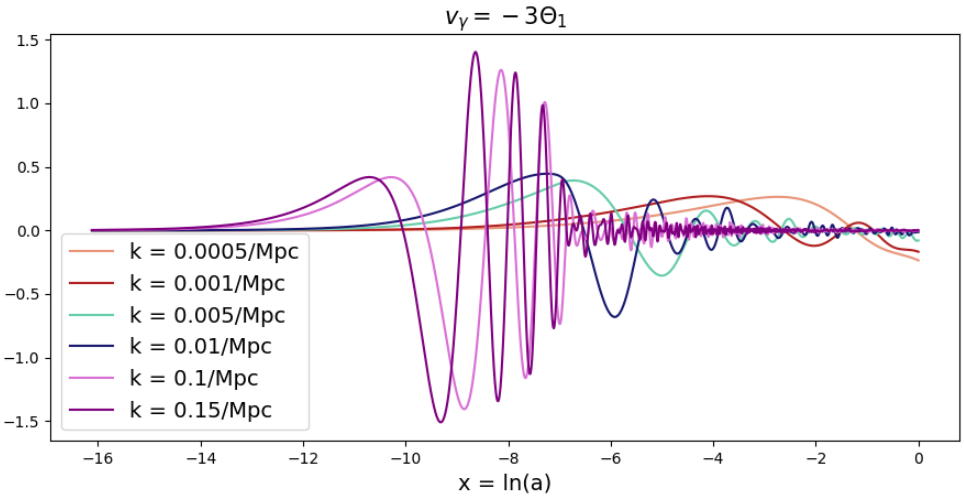

Figure 5: Perturbation to the photons - velocity, being -3 times the first multipole moment of the temperature field (dipole), $v_\gamma = -3\Theta_1$, plotted as a function of logarithm of the scale factor, x, for six different values of the wavenumber, k.

BIBLIOGRAPHY

Baumann, D. *Cosmology. Part III Mathematical Tripos.* Retrieved from: http://theory.uchicago.edu/ liantaow/my-teaching/dark-matter-472/lectures.pdf

Callin, P. (2006) *How to calculate the CMB spectrum.* Retrieved from: https://arxiv.org/pdf/astro-ph/0606683.pdf

Dodelson, S. (2003) *Modern Cosmology*, Academic Press.

Winther, H. (2020) *Overview: Milestone III.* Retrieved from: http://folk.uio.no/hansw/AST5220/notes/milestone3.html